A-6

Measurement of activation magnetic moment in ferromagnetic thin films

Sug-Bong Choe and Sung-Chul Shin

Department of Physics and Center for Nanospinics of Spintronic Materials, Korea Advanced Institute of Science and Technology, Daejon 305-701, Korea

Abstract

We have investigated the activation magnetic moment, which characterizes the basis magnetic moment acting as a single magnetic particle during magnetization reversal. The activation magnetic moment was measured from each local area on continuous ferromagnetic thin films, by analyzing the magnetic field dependence of magnetization reversal of the corresponding local area based on a thermally activated relaxation process. It was found that the activation magnetic moment was nonuniform on submicrometer scale; the fluctuation increased with increasing the number of layers in Co/Pd multilayers. The distribution could be well analyzed by $\exp(\delta m^{3/2})$, where δm is the deviation of the activation magnetic moment from the mean value.

I. Introduction

Ferromagnetic thin films and multilayers continue to be an important issue in recent years due to their novel magnetic properties as well as the possibilities of magnetoelectronic applications such as the magnetic disks, tapes, sensors, and memories [1,2]. To achieve high performance of the magnetoelectronics, it is important to characterize their dynamic properties on length scale below a micrometer as the typical dimension of magnetic elements continues to shrink to the size of the microscopic structural irregularities [3,4]. Recently, understanding on microscopic domain configurations has been greatly progressed, largely motivated by direct observations of domain structures using advanced magnetic imaging techniques with spatial resolution of some tens of nanometers [5-7]. However, despite an advantage of the high spatial resolution of the imaging techniques, dynamic studies have rarely been carried out due to the limitation imposed by applying a magnetic field and/or slow data

acquisition time.

The present study was motivated to characterize the dynamic nature of magnetization reversal on submicrometer length scale in ferromagnetic thin films. In this study, the activation magnetic moment (= magnetization M_S × activation volume V_A), which describes the basis magnetic moment acting as a single magnetic particle during magnetization reversal, has been investigated. The local activation magnetic moment was determined from each local area of 0.4×0.4 μm^2 on continuous ferromagnetic thin films, by analyzing the magnetic field dependence of magnetization reversal of the corresponding local area based on a thermally activated relaxation process. We report, for the first time, the nonuniform distribution of the activation magnetic moment during magnetization reversal in ferromagnetic thin films.

II. Experiments

A high-performance magneto-optical microscope system has been developed to directly observe the domain reversal behavior of ferromagnetic thin films having perpendicular magnetic anisotropy [8,9]. The system mainly consists of an polarizing optical microscope capable of 1,000× magnification with spatial resolution of 0.4 μm and Kerr angle resolution of 0.2 °. To trigger the domain reversal, the system is equipped with an electromagnet controlled by a personal computer to apply the external magnetic field over the range of ±3.5 kOe. The sample was first saturated by applying the magnetic field normal to the film plane and then, time-resolved domain images of 128 frames with 10 frames per second were taken under applying a reversed applied field. The domain images are captured by an advanced CCD camera system interfaced to the computer. The images are composed of the light intensity distribution measured by a CCD array of 100×80 pixels, where a unit pixel corresponds to an area of 0.4×0.4 μm^2 at the film surface. Storing the domain images during the magnetization reversal, it is possible to obtain an array of the local viscosity curves $\theta_{xy}(t)$, where t is the elapsed time after applying the reversing magnetic field. This is done by tracing the intensity variation at every corresponding $(x,y)th$ CCD pixel during the magnetization reversal under an applied magnetic field.

Fig. 1(a) shows the typical viscosity curve measured from a single CCD pixel which corresponds to an area of 0.4×0.4 μm^2 at the sample surface. It was obtained by monitoring the magneto-optical Kerr signal intensity under a constant applied magnetic field [8,10]. The figure clearly demonstrates the switching time of the magnetization

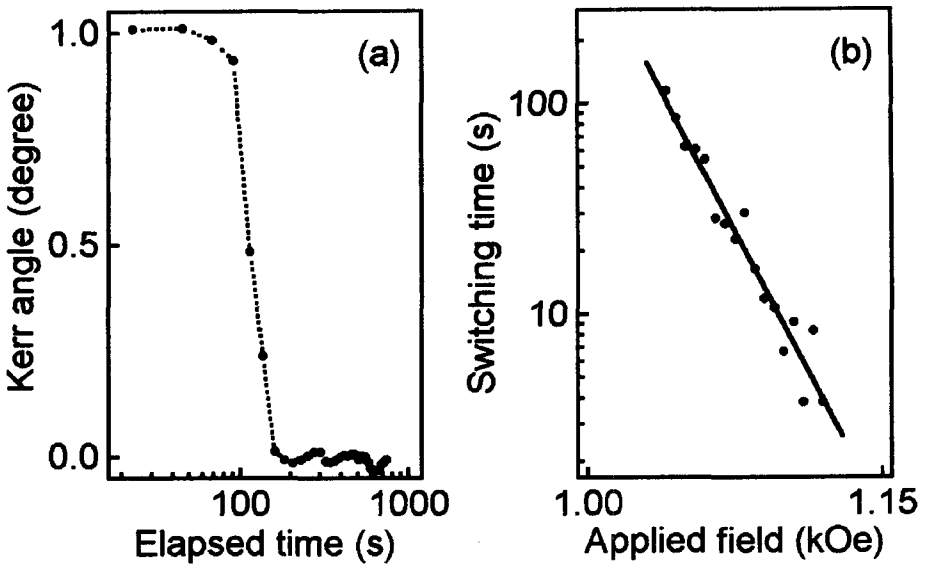

Fig. 1. (a) Typical viscosity curve measured from a CCD pixel which corresponds an area of 0.4×0.4 μm^2 at sample surface. The dotted line is guide for eyes. (b) Field dependence of the magnetization switching time of the given local area. The solid line is the best fit using Eq. (1).

of the given local area. The switching time is sensitive to the strength of the reversing applied field, and the field dependence of the switching time could be obtained from a number of observations under different applied fields near the coercivity. Fig. 1(b) illustrates the field dependence of the magnetization switching time of the given local area. It is evident in the figure that the magnetization switching time is exponentially dependent on the strength of the reversing magnetic field as shown by the solid line of the best fit [11]. The exponential dependency could be analyzed within the context of a thermally activated relaxation process:

$$\tau = \tau_0 \exp\left(\left(E_B - M_S V_A H\right)/k_B T\right), \tag{1}$$

where E_B is the switching energy barrier and τ_0 is the characteristic switching time. The equation is derived from the Neél-Brown model under an assumption of the first-order uniaxial anisotropy by linear expansion of the energy barrier with H near the experimental coercive field [12,13]. Adopting Eq. (1) as a fitting function, we could determine the activation magnetic moment m (= $M_S V_A$) from the fitting parameters.

It should be stressed here that the magnetic field dependence can be obtained for every corresponding CCD pixel and thus, one can obtain the statistics on the activation magnetic moment distribution as well as the spatial distribution map of the activation magnetic moment with a 400 nm spatial resolution.

To characterize the distribution of the activation magnetic moment in ferromagnetic thin films, Co/Pd multilayers have been chosen since they provide a variety of magnetic and/or structural properties with varying the layer structure, as well as a large polar Kerr effect for fine domain imaging. A number of $(t_{Co}\text{-Co}/t_{Pd}\text{-Pd})_n$ samples with varying either the Co-sublayer thickness t_{Co}, the Pd-sublayer thickness t_{Pd}, and the number of repeats n were prepared on glass substrates by alternatively exposing two e-beam sources of Co and Pd under a base pressure of 2.0×10^{-7} Torr at the ambient temperature [8,14]. The individual layer thickness was carefully controlled within a 4% accuracy. Low-angle x-ray diffraction studies using Cu K_α radiation revealed that all samples had distinct peaks indicating an existence of the multilayer structure. High-angle x-ray diffraction studies showed that the samples grew along the [111] cubic orientation. All samples in this study had perpendicular magnetic anisotropy and showed square Kerr hysteresis loops.

III. Results and discussion

In Fig. 2, we plot the distribution density of the local activation magnetic moment of the (2.5-Å Co/11-Å Pd)$_n$ samples. With increasing n from 5 to 15, the standard deviation Δm of the activation magnetic moment distribution increased from 2.6 to 5.2×10^{-16} emu, while the mean activation magnetic moment $\overline{m}$ decreased from 3.7 to 1.6×10^{-15} emu. It should be noticed that the distribution in magnitude is neither a Gaussian nor a Lorentzian, but surprisingly, the distribution of our samples could be well fitted by the equation of

$$\sigma = \sigma_0 \exp\left(-(\delta m / \Delta m)^{3/2}\right), \tag{2}$$

as shown by the solid lines in the figure, where σ is the distribution density and $\delta m = m - \overline{m}$. The $\delta m^{3/2}$ dependency of the activation magnetic moment distribution has been also observed for all the other Co/Pd multilayer samples having different layer structures.

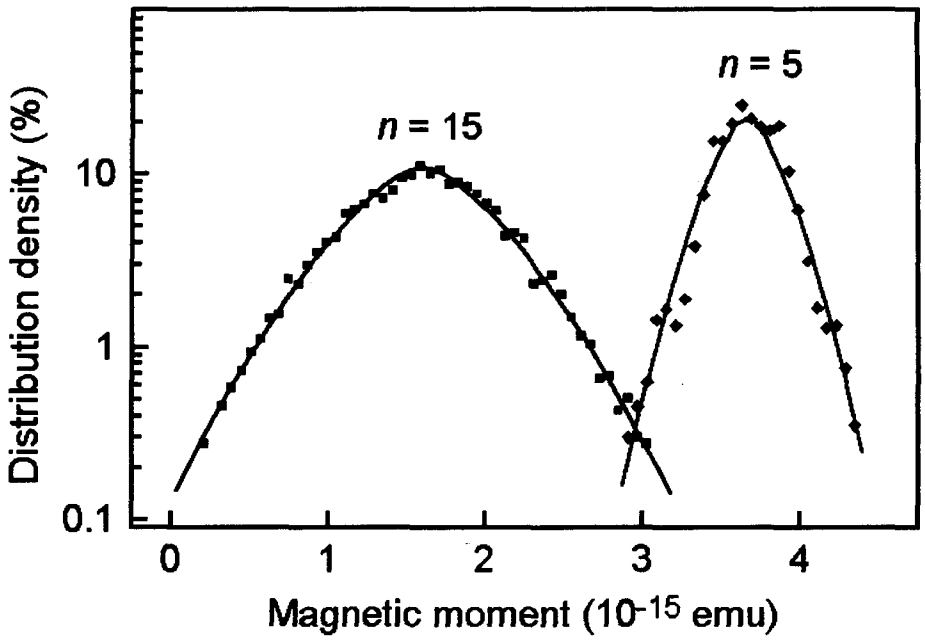

Fig. 2. Distribution density of the local activation magnetic moment of (2.5-Å Co/11-Å Pd)$_n$ multilayer samples with different number of repeats n. The density was obtained by counting the cells having the corresponding value of the local activation magnetic moment for every 6×10^{-17}-emu interval and then, normalizing by the total number of cells. The solid lines show the best fits using Eq. (2).

The most striking feature of the present measurement technique is the fact that we can generate the 2-dimensional spatial distribution map of the local activation magnetic moment variation of a sample, directly analyzing from the magnetic-field dependence of every local area simultaneously measured under an identical condition. Fig. 3 demonstrates the activation magnetic moment distributions of the (2.5-Å Co/11-Å Pd)n samples with (a) n = 5, and (b) 15, respectively. It has been done by mapping $\delta m(x,y)$ determined from the $(x,y)th$ pixel on the 2-dimensional XY plane. The values of the activation magnetic moment in several repeated measurements were confirmed to be essentially same within the experimental error. The figures vividly show the spatial fluctuation of the local activation magnetic moment on submicrometer scale. The spatial distribution of the activation magnetic moment changes with increasing n: the thinner film with n = 5 shows a smoother variation of the activation magnetic moment, while the thicker film with n = 15 shows a rougher fluctuation in the activation

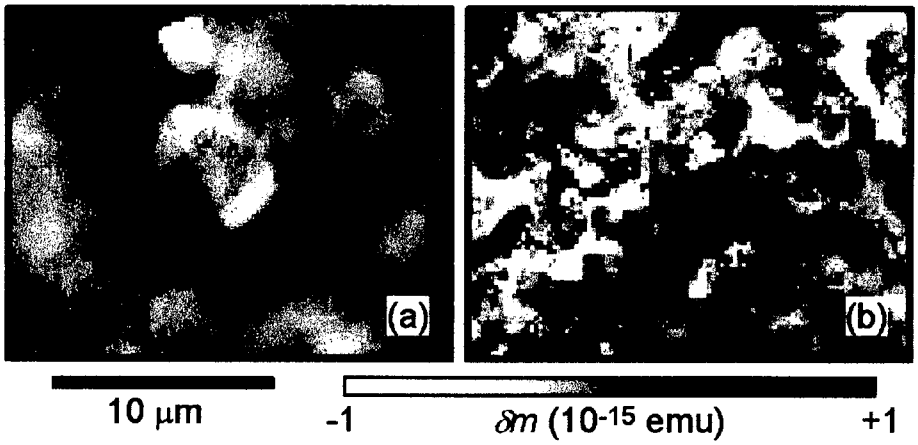

Fig. 3. Spatial distributions of the activation magnetic moment distribution of (2.5-Å Co/11-Å Pd)$_n$ multilayer samples with different number of repeats n = (a) 5 and (b) 15, respectively. The deviation delta m of the activation magnetic moment from the mean value was mapped onto the corresponding pixel having unit size of 0.4×0.4 μm^2 in gray level given by the pallet bar at the bottom of the figure. Each map corresponds to a sample surface area of 20×16 μm^2.

magnetic moment. A larger fluctuation in the activation magnetic moment of the thicker film is possibly ascribed to a larger microstructural irregularity in the thicker film [9]. AFM studies of these samples indeed revealed a tendency towards larger surface roughness with increasing n. The spatial fluctuation in the activation magnetic moment might be closely related with irregular magnetization reversal behavior observed to contrastingly change from wall-motion to nucleation dominant in Co/Pd multilayers with changing the layer structure [14]. Detailed studies on their correlation is very important to understand domain dynamics on submicrometer scale, but it is beyond the scope of this work.

IV. Conclusion

We have developed a novel technique to simultaneously determine the local activation magnetic moment from the magnetic-field dependence of the magnetization reversal observed by a magneto-optical microscope system. The activation magnetic moment

was found to be nonuniform on submicrometer scale; the distribution could be quantitatively analyzed by $\exp(\delta m^{3/2})$ and the fluctuation increased with increasing the number of layers in Co/Pd multilayers.

Acknowledgments

This work was supported by the Ministry of Science and Technology of Korea, through the Creative Research Initiatives Program.

References

[1] J. L. Simonds, Phys. Today, **48**, 26 (April 1995).
[2] K. M. Krishnan, MRS Bull. **20**, 24 (October 1995).
[3] R. P. Cowburn *et al.*, Appl. Phys. Lett. **73**, 3947 (1998).
[4] T. Aign *et al.*, Phys. Rev. Lett. **81**, 5656 (1998).
[5] E. Dan Dahlberg and J.-G. Zhu, Phys. Today, **48**, 34 (April 1995).
[6] H. Poppa, E. Bauer, and H. Pinkvos, MRS Bull. **20**, 38 (October 1995).
[7] R. Wiesendanger *et al.*, Phys. Rev. Lett. **65**, 247 (1990).
[8] S.-B. Choe and S.-C. Shin, Phys. Rev. B, **57**, 1085 (1998).
[9] S.-B. Choe and S.-C. Shin, Phys. Rev. B, *in press* (2000).
[10] M. Labrune *et al.*, J. Magn. Magn. Mater. **80**, 211 (1989).
[11] S.-B. Choe and S.-C. Shin, J. Appl. Phys. **87**, 5076 (2000).
[12] L. Neél, Ann. Geophys. **5**, 99 (1949);W. F. Brown, Phys. Rev. **130**, 1677 (1963).
[13] J. Pommier *et al.*, Phys. Rev. Lett. **65**, 2054 (1990).
[14] S.-C. Shin and S.-B. Choe, IEEE Trans. Magn. **35**, 3853 (1999).